International Journal of Biochemistry and Cell Biology 110 (2019) 91–102

Contents lists available at ScienceDirect

International Journal of Biochemistry and Cell Biology

journal homepage: www.elsevier.com/locate/biocel

LPA_1 receptor activation induces PKCα nuclear translocation in glioblastoma cells

Silvia Anahi Valdés-Rives[a], Marisol de la Fuente-Granada[a], Marco A. Velasco-Velázquez[b,c], Oscar González-Flores[d,e], Aliesha González-Arenas[a,*]

[a] Departamento de Medicina Genómica y Toxicología Ambiental, Instituto de Investigaciones Biomédicas, Universidad Nacional Autónoma de México, Ciudad de México, Mexico
[b] Departamento de Farmacología y, Facultad de Medicina, Universidad Nacional Autónoma de México, Ciudad de México, Mexico
[c] Unidad Periférica de Investigación en Biomedicina Traslacional (C.M.N. 20 de noviembre, ISSSTE), Facultad de Medicina, Universidad Nacional Autónoma de México, Ciudad de México, Mexico
[d] Centro de Investigación en Reproducción Animal, Universidad Autónoma de Tlaxcala-CINVESTAV, Tlaxcala, Mexico
[e] Área de Neurociencias, Departamento de Biología de la Reproducción, CBS, UAM-I, Ciudad de México, Mexico

ARTICLE INFO

Keywords:
Glioblastoma
LPA
LPA_1 receptor
PKCα
Nucleus

ABSTRACT

Lysophosphatidic acid (LPA) is a ubiquitous lysophospholipid that induces a wide range of cellular processes such as wound healing, differentiation, proliferation, migration, and survival. LPA signaling is increased in a number of cancers. In Glioblastoma (GBM), the most aggressive brain tumor, autotaxin the enzyme that produces LPA and its receptor LPA_1 are overexpressed. LPA_1 is preferentially couple to $G\alpha_q$ proteins in these tumors that in turn activates PKCs. PKCs are involved in many cellular processes including proliferation and metastasis. In this study, we aimed to determine if a classical PKC (α isozyme), could be activated through LPA_1 in GBM cell lines and if this activation impacts on cell number. We found that LPA_1 induces PKCα translocation to the nucleus, but not to the cell membrane after LPA treatment and the cell number diminished when LPA_1/PKCα signaling was blocked, suggesting a relevant role of LPA_1 and PKCα in GBM growth.

1. Introduction

Lysophosphatidic acid (LPA) is a small lysophospholipid that consists of an acyl chain at the sn-1 (or sn-2) position of a glycerol backbone and a phosphate head group (Mooleenar, 2006). It acts through six GPCRs named $LPA_{1\text{-}6}$ that are coupled to Gα proteins: $G\alpha_{q/11}$, $G\alpha_{i/0}$, $G\alpha_{12/13}$, $G\alpha_s$. Consequently, depending on cellular context, LPA can exert a wide range of physiological effects such as wound healing, differentiation, neurogenesis, and survival (Yung et al., 2015; Gonzalez-Gil et al., 2015). LPA is mainly produced by autotaxin (ATX) a 125kDa-secreted enzyme from the family of ectonucleotide pyrophosphatases/phosphodiesterases (Perrakis and Moolenaar, 2014). ATX generates LPA from plasma membrane phospholipids and from circulating lysophosphatidylcholine (LPC) bound to albumin (Zhang et al., 2009). Due to the small nature of LPA, it is water soluble, and different concentrations of this lysophospholipid have been reported in body fluids.

Aberrant ATX-LPA signaling has been linked to some pathologies namely inflammation, autoimmunity, neurological disorders, fibrosis, and cancer (Valdés-Rives and González-Arenas, 2017; Yung et al., 2014). In several malignancies, ATX expression and LPA concentrations are elevated, i.e., LPA can reach up to 80μM in ascites fluid from ovarian cancer (Yung et al., 2014; Mills and Moolenaar, 2003; Benesch et al., 2014), while in non-pathological conditions concentrations around 5μM have been reported in serum plasma (Yung et al., 2014; Mills and Moolenaar, 2003; Choi and Chun, 2013).

Moreover, the LPA_1 receptor has been linked to malignant progression by enhancing proliferation, migration, angiogenesis, and cancer stem-cell maintenance in some tumors such as breast cancer, pancreatic cancer, ovarian cancer, and glioblastoma (Zhang et al., 2009; Lee et al., 2015; Seo et al., 2016; Fukushima et al., 2017).

Glioblastoma (GBM), also known as an astrocytoma grade IV, represents the maximal evolution stage of astrocytomas and it is among the most lethal human malignancies (Louis et al., 2007; Ostrom et al., 2018). The median survival for GBM patients, with the best therapy, is

* Corresponding Author at: Departamento de Medicina Genómica y Toxicología Ambiental, Instituto de Investigaciones Biomédicas, Universidad Nacional Autónoma de México, Ciudad Universitaria, 04510, Ciudad de México, Mexico.
E-mail addresses: anahiivaldes@gmail.com (S.A. Valdés-Rives), mdelafuente@iibiomedicas.unam.mx (M. de la Fuente-Granada), marcovelasco@unam.mx (M.A. Velasco-Velázquez), oglezflo@gmail.com (O. González-Flores), alieshagonzalez@gmail.com (A. González-Arenas).

https://doi.org/10.1016/j.biocel.2019.03.003
Received 27 June 2018; Received in revised form 6 February 2019; Accepted 4 March 2019
Available online 05 March 2019
1357-2725/

12–15 months, and only 3–5% of the patients survive for more than three years. In the Mexican population, it has been estimated that the mean age of incidence is 45 ± 15 years, compared to the global estimate of 60 ± 15 years (Wegman-Ostrosky et al., 2016; Louis et al., 2016).

A recent study showed that primary cilium regulates LPA_1 signaling in astrocytes, and the loss of the cilium induced an increased proliferation in an LPA-dependent manner in these cells (Loskutov et al., 2018). In GBM, the primary cilia are lost, and LPA_1 is redistributed in the cell membrane enhancing a signaling pathway to induce malignant progression. Moreover, ATX and LPA_1 are augmented in GBM, and LPA_1 increases its coupling to $G\alpha_q$ and $G\alpha_{12}$ proteins (Loskutov et al., 2018; Kishi et al., 2006; Tabuchi, 2015; Steinberg, 2008). $G\alpha_q$ proteins activate phospholipase C (PLC), which in turn produces diacylglycerol (DAG) and inositol 1,4,5-trisphosphate (IP3) from phosphatidylinositol 4,5-bisphosphate (PIP2) (Koivunen et al., 2006; Steinberg, 2008). DAG activates classic and novel PKCs, serine/threonine kinases.

The role of PKCs in cancer progression is well-known (do Carmo et al., 2013). In GBM, PKCα is the most expressed among these kinases (Koivunen et al., 2006; Mandil et al., 2001). PKCα is known to induce a proliferative and pro-survival effect in GBM (Cameron et al., 2008; González-Arenas et al., 2015), but since this kinase has a wide variability of actions its contribution through specific signaling pathways for the development of GBM is poorly understood, and its target in therapy has ended in failure (do Carmo et al., 2013). Therefore, we aimed to study the activation of PKCα through the stimulation of LPA_1 to understand one of the mechanisms through which these two molecules participate in glioblastoma biology.

2. Materials and methods

2.1. Cell Culture and treatments

All cell lines were culture in DMEM medium (In Vitro, Mex), supplemented with 10% fetal bovine serum (FBS) at 37 °C under a 95% air and 5% CO_2 atmosphere. CaCo2 needs 20% of (FBS). Cell lines used: human GBM derived cell lines U251, U87 and LN229 (American Type Culture Collection, USA); human ovarian cancer-derived cell line SKOV3 (American Type Culture Collection, USA); human colon cancer-derived cell lines CaCo2 and HCT-116 (American Type Culture Collection, USA). Tetradecanoyl phorbol acetate (TPA; Sigma-Aldrich, USA) was used to activate PKCα. 1-Oleoyl Lysophosphatidic Acid (LPA; Cayman Chemical, USA) was used to activate LPA receptors. LPA_1 antagonist Ki16425 (Sigma-Aldrich, USA) was added 30 min before the LPA treatment when used.

2.2. Cellular fractionation

10×10^6 cells were maintained as described in the *Cell culture and treatments*. Twelve hours before treatments, the medium was changed for phenol red-free DMEM without fetal bovine serum. After treatments, cells were homogenized in ice-cold Buffer A with protease inhibitors (20 mM Tris−HCl, 0.25 M sucrose, 2 mM EDTA and 2 mM EGTA in distilled water, pH = 7.5). The cell suspension underwent one freeze-thaw cycle in dry ice. The samples were centrifuged at 2800 x *g* at 4 °C for 10 min. The pellets (nuclear fraction) were resuspended in 200 µL of Buffer A and stored until used. The supernatant was centrifuged at 200,000 x *g* at 4 °C for 105 min using an ultracentrifuge. The supernatant (cytosol) was stored until used. The pellet was resuspended in ice-cold Buffer B with protease inhibitors (20 mM Tris−HCl, 1 mM EDTA, 1 mM EGTA, 150 mM NaCl, and 1% Triton X-100 in distilled water, pH = 7.5) and centrifuged at 16,000 x *g* at 4 °C for 15 min. The supernatant (Membrane fraction) was stored until used. Proteins were quantified using a NanoDrop 2000 Spectrophotometer (Thermo Scientific, USA).

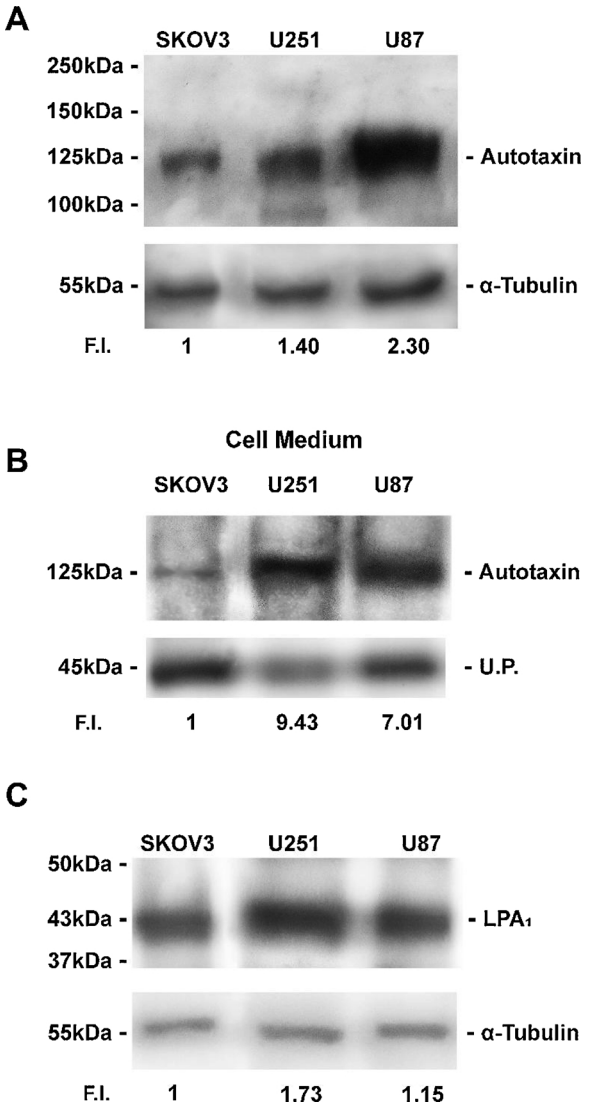

Fig. 1. Glioblastoma cell lines highly express autotaxin and LPA_1. A) Representative Western Blot for autotaxin content in glioblastoma cell lines (U251 and U87) and SKOV3. B) Representative Western Blot for AXT secreted to the cell medium in glioblastoma cell lines (U251 and U87) and SKOV3. U.P.: unspecific protein taken for quantification purposes. C) Representative Western Blot for LPA_1 content in glioblastoma cell lines (U251 and U87) and SKOV3. F.I. (Fold increase). All blots are representative of two independent experiments.

2.3. Western blotting

Nuclear (100 µg), cytosolic (50 µg) and membrane (50 µg) proteins were separated by electrophoresis on 10% and 7.5% SDS-PAGE gels respectively at 20 mA. Colored markers (Bio-Rad, USA) were included for size determination. Gels were transferred to nitrocellulose membranes (Millipore, USA) for 2 h (60 mA, at room temperature in semi-dry conditions). The membranes were blocked with 5% nonfat dry milk and 2% bovine serum albumin at room temperature for 2 h. Membranes were incubated with an antibody against PKCα (0.66 µg/mL; sc-8393; Santa Cruz Biotechnology, USA) at 4 °C overnight. Blots were then incubated with an anti-mouse secondary antibody (1:5000) conjugated to horseradish peroxidase (Santa Cruz Biotechnology, USA) for 45 min. To correct for differences in the amount of total protein loaded in each lane, PKCα content in the nuclear fraction was normalized to that of histone 3 (H3), PKCα content in the cytosolic fraction was normalized to that of α-tubulin, and PKCα content in the membrane fraction was normalized to that of glucose transporter, Glut3. Blots were stripped

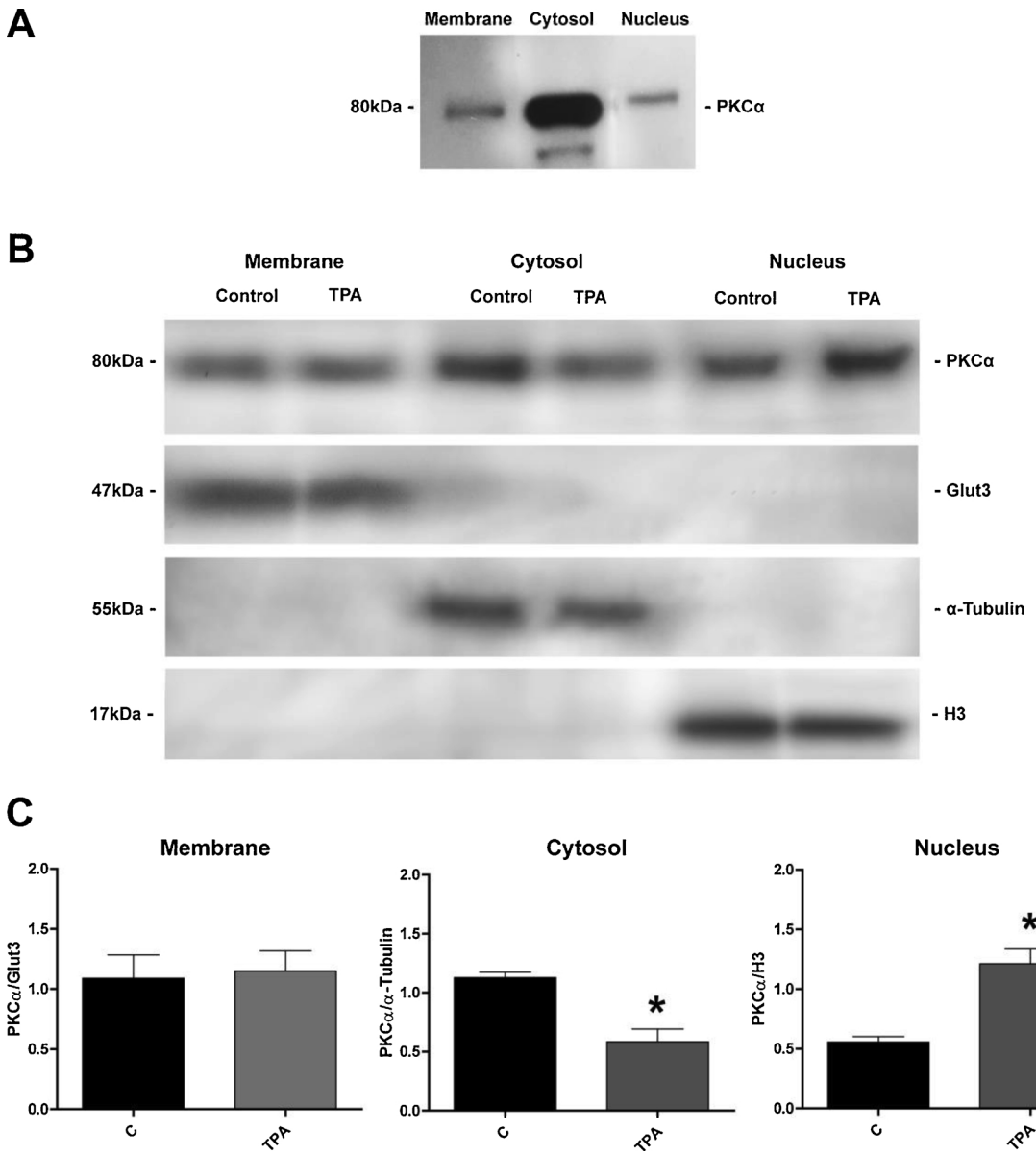

Fig. 2. TPA induces PKCα translocation to the nucleus. A) Representative western blot of PKCα cellular distribution under non-stimulus conditions in different cell fractions of U251 cell line. B) Representative western blots of PKCα content in the cell membrane, cytosol, and nucleus after 5 min of TPA (1μM) stimulation (Control (C): DMSO 10%); Glut 3 transporter, α-tubulin, and histone H3 were used as specific proteins for each compartment. C) Graphic representation of 3 independent experiments. PKCα from each compartment was compared to its specific protein for quantification. Results are expressed as the mean + S.E.M., Bonferroni post-test determined statistical difference, *$p < 0.05$ versus control.

with glycine [0.1 M, pH 2.5; 0.5% sodium dodecyl sulfate (SDS)] at 4 °C overnight and at room temperature for 30 min. Then they were re-probed with 0.1 μg/mL of rabbit anti-histone 3 polyclonal antibody (06-599-MN; Merck Millipore, USA), 0.4 μg/mL of mouse anti-α-tubulin monoclonal antibody (sc-398103; Santa Cruz Biotechnology, USA), 0.66 μg/mL of mouse anti-Glut3 monoclonal antibody (sc-74399; Santa Cruz Biotechnology, USA) respectively at 4 °C overnight. Blots were then incubated with an anti-mouse secondary antibody (1:15,000; Abcam, USA), or an anti-rabbit secondary antibody (1: 12,000; Santa Cruz Biotechnology, USA) conjugated to horseradish peroxidase at room temperature for 45 min. Chemiluminescence signals were detected exposing the membranes to Kodak Biomax Light Film (Sigma-Aldrich, USA) using Supersignal West Femto as peroxidase substrate (Thermo Scientific, USA). Detection of the LPA_1 receptor, LPA_3 receptor, and ATX was done in whole cells under control conditions homogenized in RIPA lysis buffer with protease inhibitors (1 mM EDTA, 2 μg/mL leupeptin, 2 μg/mL aprotinin, 1 mM phenylmethylsulphonyl fluoride). Proteins were obtained by centrifugation at 12,500 rpm, at 4 °C for 15 min and quantified using a NanoDrop 2000 Spectrophotometer (Thermo Scientific, USA). Proteins (100 μg) were determined by Western blotting. Blots were incubated with 3 μg/mL LPA_1 rabbit polyclonal antibody (ab23698; Abcam, USA), 1 μg/mL LPA_3 mouse monoclonal antibody (sc-390270; Santa Cruz Biotechnology, USA) and 0.2 μg/mL ATX mouse monoclonal antibody (sc-374222; Santa Cruz Biotechnology, USA). To correct for differences in the amount of total protein loaded in each lane the content was normalized to that of α-tubulin as described above.

2.4. Immunofluorescence

8,000 cells per well were plated in Millicell EZ 4-well glass slides (Millipore, USA). Eighteen hours before treatments, the medium was

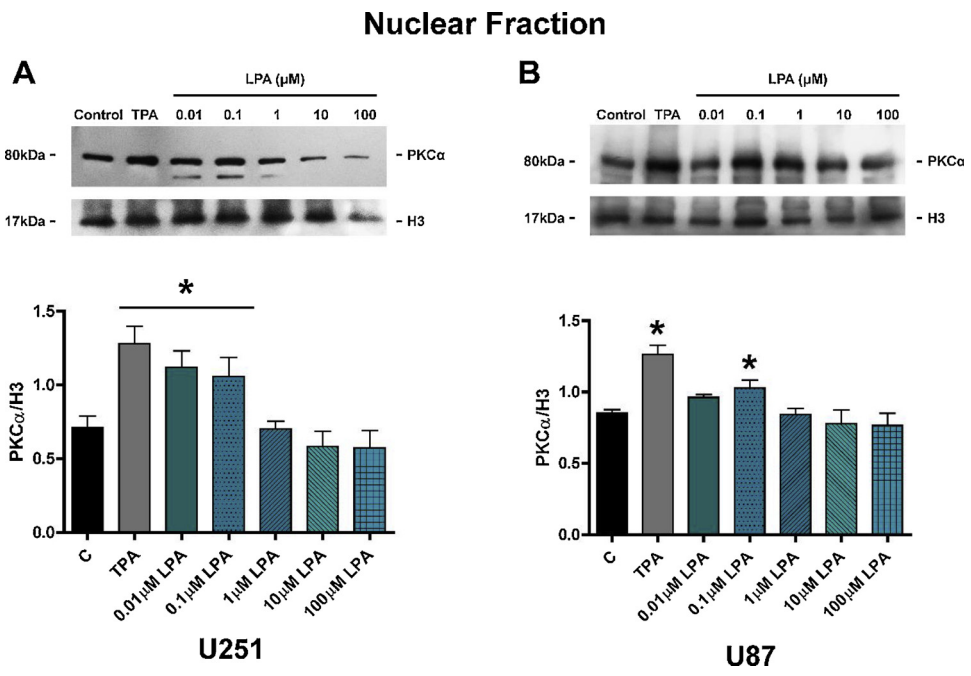

Fig. 3. LPA induces PKCα nuclear translocation in glioblastoma cells. Cell lines were treated with TPA (1μM) or different LPA concentrations (0.01 μM–100 μM) for 5 min in U251 (A) or U87 (B). Upper panels: Representative Western Blots of nuclear fractions, Bottom panels: Graphic representation of 3 independent experiments. Results are expressed as the mean ± S.E.M., Bonferroni post-test determined statistical difference *$p < 0.05$ versus the control.

changed for phenol red-free DMEM without fetal bovine serum. After the treatments, cells were fixed for 20 min in 4% paraformaldehyde solution at 37 °C and permeabilized with 100% methanol for 6 min at -4 °C. Next, fixed cells were blocked with 1% bovine serum albumin in PBS for 1 h at room temperature and incubated at 4 °C for 24 h with 1 μg/mL of monoclonal mouse antibody anti-PKCα (sc-8393; Santa Cruz Biotechnology, USA) in 0.5% bovine serum albumin in PBS. The samples were rinsed thrice in PBS for 5 min each and incubated in the dark with anti-mouse Alexa Fluor 594-labeled secondary antibodies (Invitrogen, USA) for 45 min. Nuclei were stained with 1 μg/mL Hoechst 33,342 solution (Thermo Scientific, USA), and the cells were coverslipped with fluorescence mounting medium (Biocare Medical, USA). To detect Alexa Fluor 594 and Hoechst fluorescence the samples were visualized in an Olympus B × 43 F microscope using different wavelengths to excite the fluorochromes. Photographs were taken at 60x magnification. To establish colocalization of the detected signals merged images were generated using ImageJ software (National Institutes of Health, USA). The examiner was unaware of the treatment conditions of the cells. Isotype controls were performed for all immunofluorescence (data not shown). For nuclear PKCα quantification, the samples were visualized in a Nikon A1R + STORM confocal microscope. The nuclear PKCα stain was quantified using ImageJ software (National Institutes of Health, USA). The DAPI images were used to select the nuclei, and the area was an overlay in the PKCα channel. The fluorescence was divided by the nuclear area to obtain a mean fluorescence intensity per nucleus.

2.5. Viability assay

15,000 cells per well were plated in a 24-well plate. DMEM with 10% of FBS was used for this assay. The cells were treated for 24 h with Ki16425 2.5 or 5 μM. Cells were detached with PBS-EDTA, and the cell suspension was stained with Trypan Blue (T-6146, Sigma, USA). Cell number was first determined in a Neubauer chamber. The percentage of viable cells was calculated by diving the number of viable cells by the number of total cells and multiplying by 100.

2.6. Cell transfection with siRNAs

Specific small interfering RNAs (siRNAs) (Santa Cruz Biotechnology) were used to inhibit the expression of PKCα (sc-36423). Control siRNA has a scramble sequence that does not lead to the specific degradation of any known cellular mRNA. U251, U87, and LN229 were grown in six-well plates to a confluence of 60% and then were transfected with 0.35 nM of siRNA using Lipofectamine 2000 (Invitrogen, Life Technologies) as described by the manufacturer. To confirm PKCα silencing, a western blot for the enzyme were carried out in cell lysates after 72 h of siRNA transfection.

2.7. Flow cytometry

To assess phosphorylation of PR at S400 intracellular staining was performed. Immediately after the stimulation of times indicated, cells were collected, fixed with PBS/Paraformaldehyde 2% at 37 °C for 10 min, and permeabilized with ice-cold methanol at 4 °C for 30 min. Then, cells were washed with FACs buffer (PBS/4% fetal bovine serum) and incubated with blocking solution (FACs buffer/10% goat serum) for 20 min at 4 °C using goat serum. After blockage, cells were stained by using 0.5 μg/50 μl of rabbit anti-pS400PR (ab60954, Abcam, USA) at 4 °C for 20 min and washed with FACs buffer. Cells were then incubated with secondary goat anti-rabbit IgG-AF488 antibody by using 0.5 μg/50 μl (A11034, Invitrogen, USA) at 4 °C for 30 min, protected from light. Cells were washed and resuspended in FACs buffer. Samples were acquired in an Attune Acoustic Focusing Flow Cytometer (Life Technologies, USA) and analyzed using FlowJo 10.0 software (Tree Star Inc., USA).

Specific characteristics of the antibodies described in sections *2.3, 2.4* and *2.5* can be consulted in Supplementary Table 1.

2.8. Statistical analysis

All data were analyzed and plotted using the GraphPad Prism 5.0 software for Windows XP (GraphPad Software, USA). Statistical analysis of comparable groups was performed using a one-way ANOVA with a Bonferroni posttest. A value of $P = 0.05$ or less was considered statistically significant as stated in figure legends.

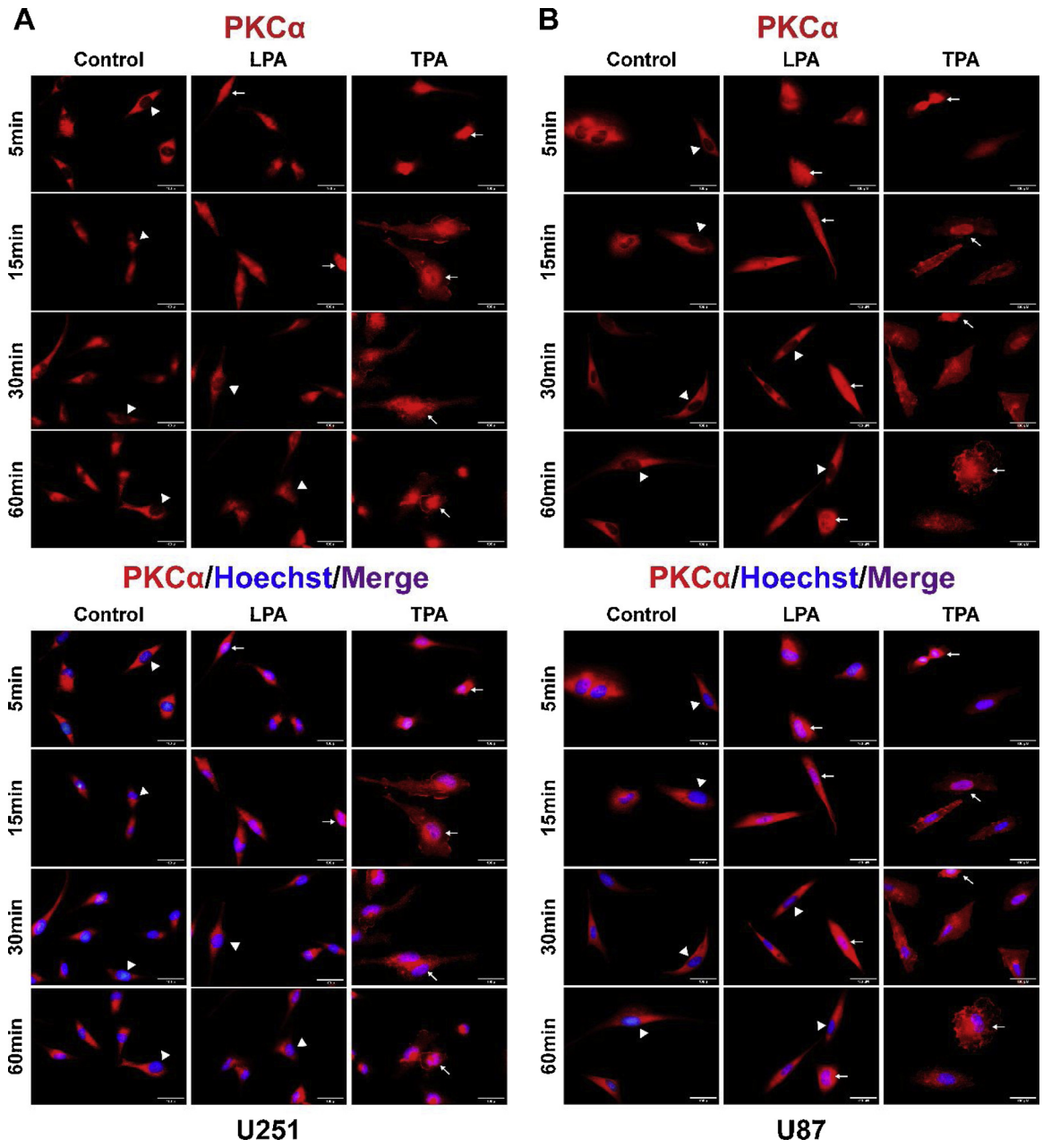

Fig. 4. Temporal translocation of PKCα induced by LPA and TPA in glioblastoma cells. Translocation of PKCα with respect to time in A) U251 and B) U87 cells treated with LPA (100 nM) and TPA (1μM). Top: PKCα (Red), Bottom: Hoechst (Blue), Merge (Purple). Representative images of 3 independent experiments. Photographs were taken at 60x magnification. Scale bar = 100 μm. Arrowheads indicate empty nucleus, arrows indicate occupied nucleus with PKCα. Just one arrowhead or arrow per image are shown not to saturate the pictures (For interpretation of the references to colour in this figure legend, the reader is referred to the web version of this article).

3. Results

3.1. GBM-derived cell lines express autotaxin and LPA1

ATX enzyme is the main pathway by which LPA is produced in physiological and some pathological conditions. Our results show a 2.30 and 1.40 fold increase in ATX content in U87 and U251 respectively compared with SKOV3 (Fig. 1A), an ovarian cell line that highly express this enzyme and LPA_1 receptor (Seo et al., 2016; Kishi et al., 2006). We also evaluated ATX secretion in these cell lines, U251 and U87 presented a 9.43 and 7-fold increase respectively of secreted ATX compared to SKOV3 (Fig. 1B).

LPA_1 content was also augmented in U251 and U87 cells (1.73 and 1.15-fold increase, respectively) compared with SKOV3 protein content (Fig. 1C).

The expression of ATX and LPA receptors have been reported before for U251 and U87 cell lines at a mRNA level (Kishi et al., 2006; Lee et al., 2008), but have not been demonstrated at a protein level, as has been done in this work.

3.2. Low concentrations of LPA induce PKCα nuclear translocation

To evaluate the effect of LPA on PKCα activation by kinase translocation, first, we assessed a positive control of PKCα activation, 12-O-Tetradecanoylphorbol-13-acetate (TPA). GBM cells were treated with TPA 1μM, and after 5 min of stimulation, PKCα translocation was measured in the cell membrane, cytoplasm, and nucleus. Our results show that PKCα is mainly located in the cytoplasm under no

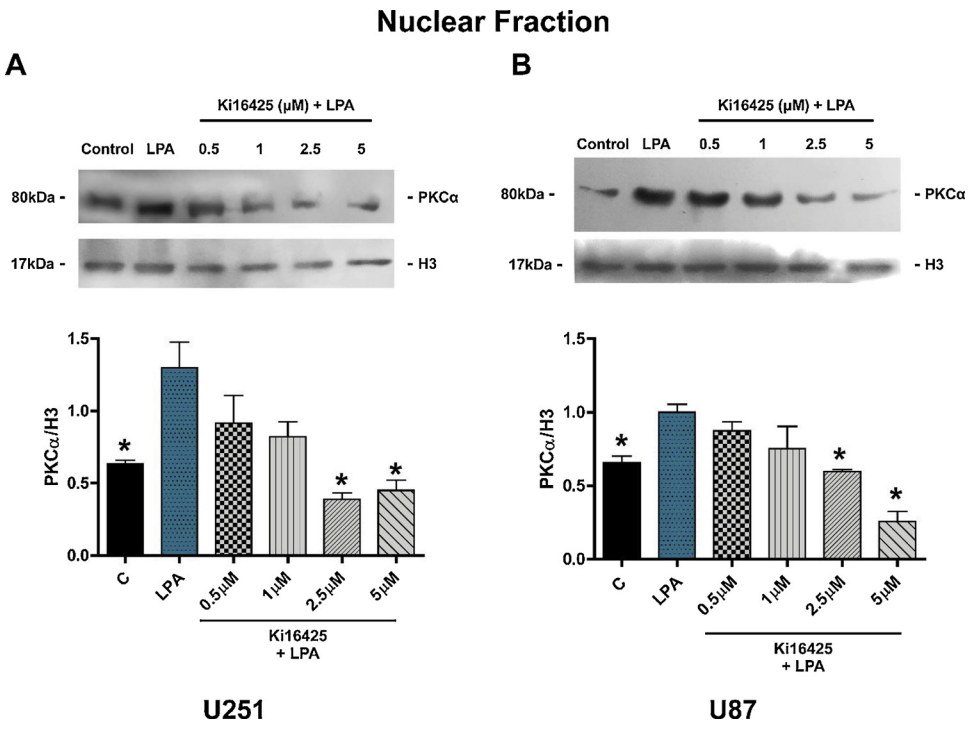

Fig. 5. Ki16425 at increasing concentrations antagonizes LPA effect on PKCα translocation. Cells treated with increasing concentrations of Ki16425 inhibits PKCα translocation to the nucleus in A) U251 and B) U87 after 5 min of LPA (100 nM) stimulation. Upper panels: Representative Western Blot, Bottom panel: Graphic representation, results are expressed as the mean + S.E.M of 3 independent experiments. Bonferroni post-test determined statistical difference *$p < 0.05$ versus LPA.

stimulation (Fig. 2A), but strongly translocated to the nucleus at 5 min with TPA, and not to the cell membrane in glioblastoma cells (Fig. 2B-C).

To study if PKCα translocation induced by LPA is like the one produced by TPA, first, we tested the effect of different LPA concentrations (Fig. 3). Interestingly, in U251 concentrations of 10 and 100 nM of LPA induced a significant PKCα translocation to the nucleus compared to the control, while in U87 PKCα translocation was achieved at 100 nM of LPA. We also evaluated the content of PKCα in the cytosol, which showed the opposite result (Supplementary Fig. 1). Low concentrations of LPA diminished PKCα content in the cytosol, while higher concentration maintained the content similar to the control in this cell fraction. It is worth noting that 1,10, and 100μM of LPA did not promote a PKCα translocation to the cell membrane at 5 min of stimulation (Supplementary Fig. 2).

3.3. LPA does not induce PKCα membrane translocation in GBM in a time-dependent manner

PKCα is known to translocate to the cell membrane after activation. We were interested in studying if this translocation was time-dependent in LPA activation. Therefore, we evaluated the effect of 100 nM LPA on PKCα translocation at 5, 15, 30, and 60 min. We chose 100 nM LPA since it elicited a similar nuclear translocation of PKCα in both cell lines. We decided to compare LPA effect with TPA because in many PKCα studies it is the most common activator used to understand this kinase effects on cellular biology.

Remarkably, the effect on PKCα translocation through time differs depending on its activator (Fig. 4). LPA induced the kinase nuclear translocation at 5 and 15 min in both cell lines, which was later redistributed to the cytoplasm at 30 and 60 min but with no accumulation at the cell membrane. On the other hand, TPA induced a robust translocation of the protein to the nucleus at 5 min after treatment. However, at 15, 30 and 60 min of stimulation, while some PKCα could be detected in the nucleus, it was also redistributed to the cytoplasm and the cell membrane. Our results show that LPA promotes a PKCα nuclear translocation, not a membrane translocation, in glioblastoma cell lines.

3.4. Ki16425 inhibits PKCα nuclear translocation in GBM

As already mentioned, LPA can induce its effects through several GPCRs. To determine if the results obtained were elicited through LPA_1, we used an LPA_1/LPA_3 antagonist Ki16425.

To determine the optimal concentration of Ki16425 to inhibit PKCα nuclear translocation, we evaluated the effect of the antagonist at different concentrations after 5 min of stimulation with LPA 100 nM (Fig. 5). We also assessed the kinase content in the cytosol at different concentrations of the antagonist (Supplementary Fig. 3). Our results determined that 2.5μM and 5μM of Ki16425 inhibit PKCα nuclear translocation in glioblastoma cell lines.

We have shown that PKCα nuclear translocation occurs at 5–15 min after stimulation with LPA (Fig. 4), we decided to test the inhibition of PKCα translocation at 15 min with Ki16425 (Fig. 6). We chose to study this signaling pathway by adding a third cell line (LN229) to see if it will be a conserved pathway in different GBM cell lines. LN229 also expresses ATX and LPA_1 similarly to U251, but PKCα has a lower content in comparison to U251 and U87 (Supplementary Fig. 4).

LPA_3 receptor content was analyzed in all glioblastoma cell lines since this protein has not been previously reported in these cells and could contribute to the effects of LPA shown in this study. U251 and U87 cell lines did not express LPA_3, while LN229 expresses this receptor as HCT116, a colon carcinoma cell line, positive to this receptor. CaCo2, a cell line that has been reported negative to LPA_3, was used as a negative control (Supplementary Fig. 5) (Leve et al., 2015).

Our results show that in U251 and U87 cell lines, LPA induces PKCα translocation to the nucleus meanwhile Ki16425, an antagonist for LPA_1, blocks this effect. On the other hand, LN229 has PKCα distributed in both cytosol and nucleus in control conditions, but LPA stimulation concentrates this kinase in the nucleus and Ki16425 treatment blocks this effect in these cells.

Moreover, we decided to quantify the translocation of PKCα to the nucleus in U87 cells after stimulation with LPA 100 nM and/or Ki16425 2.5 μM (15 min) using confocal microscopy (Fig. 7).

The results showed that LPA 100 nM after 15 min induces a significant translocation of PKCα to the nucleus compared to control and the LPA_1 receptor antagonist, Ki16425, blocks this effect even when

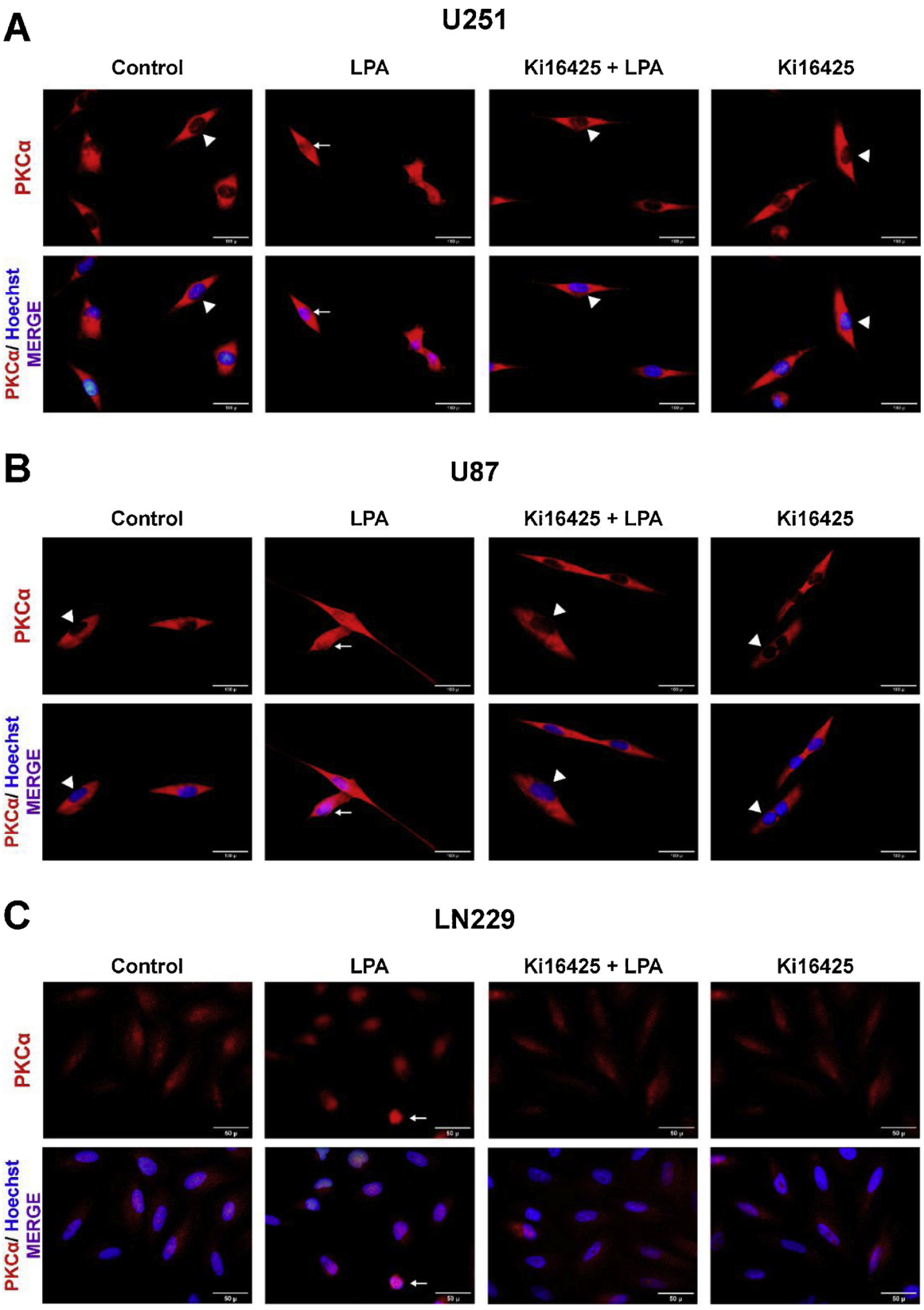

Fig. 6. LPA_1 mediates LPA effect on PKCα translocation. Cells treated with Ki16425 (2.5μM) inhibits LPA (100 nM) effect on PKCα nuclear translocation at 15 min of stimulation in all glioblastoma cells lines A) U251, B) U87 and C) LN229. PKCα (Red), Hoechst (Blue), Merge (Purple). Representative images of 3 independent experiments. Photographs were taken at 60x magnification. Scale bars: 100 μm for U251 and U87, 50 μm for LN229. Arrowheads indicate empty nucleus, arrows indicate occupied nucleus with PKCα. Just one arrowhead or arrow per image are shown not to saturate the pictures (For interpretation of the references to colour in this figure legend, the reader is referred to the web version of this article).

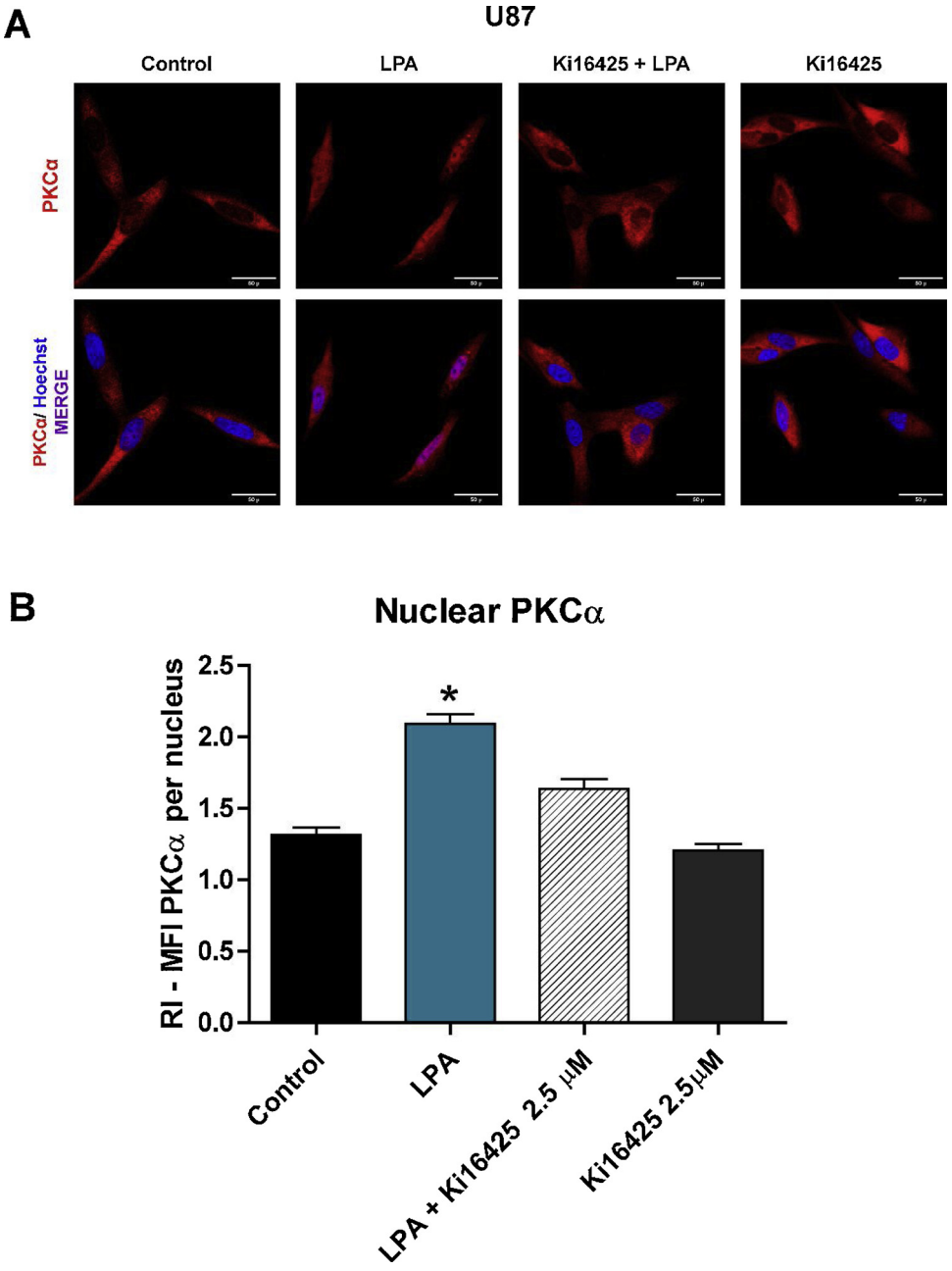

Fig. 7. Nuclear PKCα quantification. A) Representative images of confocal microscopy of U87 cells stimulated with LPA 100 nM and/or Ki16425 2.5 μM. B) Graphic representation, results are expressed as the mean + S.E.M of 3 independent experiments, 150 nuclei cells were quantified per treatment. Bonferroni post-test determined statistical difference *p < 0.05 versus control, LPA + Ki16425 and Ki16425. Photographs were taken at 20x magnification with a 3.62 zoom in a Nikon A1R + STORM confocal microscope. Scale bar = 100 μm.

LPA is added. These results demonstrate that nuclear translocation of PKCα induced by LPA is mediated through its LPA_1 receptor.

3.5. LPA1/PKCα inhibition decreases cell number in GBM

To confirm that PKCα translocation induced by LPA resulted in meaningful changes in cell proliferation, we evaluate the role of LPA_1 and PKCα on cell number and viability of glioblastoma cell lines. These assays were performed in the presence of 10% of FBS as the source of LPA, that is an abundant component of serum (Gaits et al., 1997; Li et al., 2003).

After 24 h of treatment with Ki16425 to antagonize LPA_1 receptor activity, all cell lines showed a decrease in cell number (Fig. 8A) and only U251 cell line showed a reduction in viability at this time (Fig. 8B). To further study the impact of PKCα on cell number and viability, we silenced the expression of this kinase with a siRNA in the three cell lines, we observed that PKCα silencing decreased cell number but not viability in U87 and LN229 cell lines (Fig. 9A and B). However, in U251 cell line both processes were diminished (Fig. 9A and B), this may imply that in these cells LPA_1 and PKCα are relevant for proliferation and survival. Both treatments in the three cell lines did not have a synergistic or additive effect on cell number or viability (Fig. 9A and B) suggesting that LPA_1 and PKCα are in a common pathway.

3.6. LPA induces the phosphorylation of the progesterone receptor in the residue serine 400 (S400)

Previously, our group has demonstrated that PKCα phosphorylates

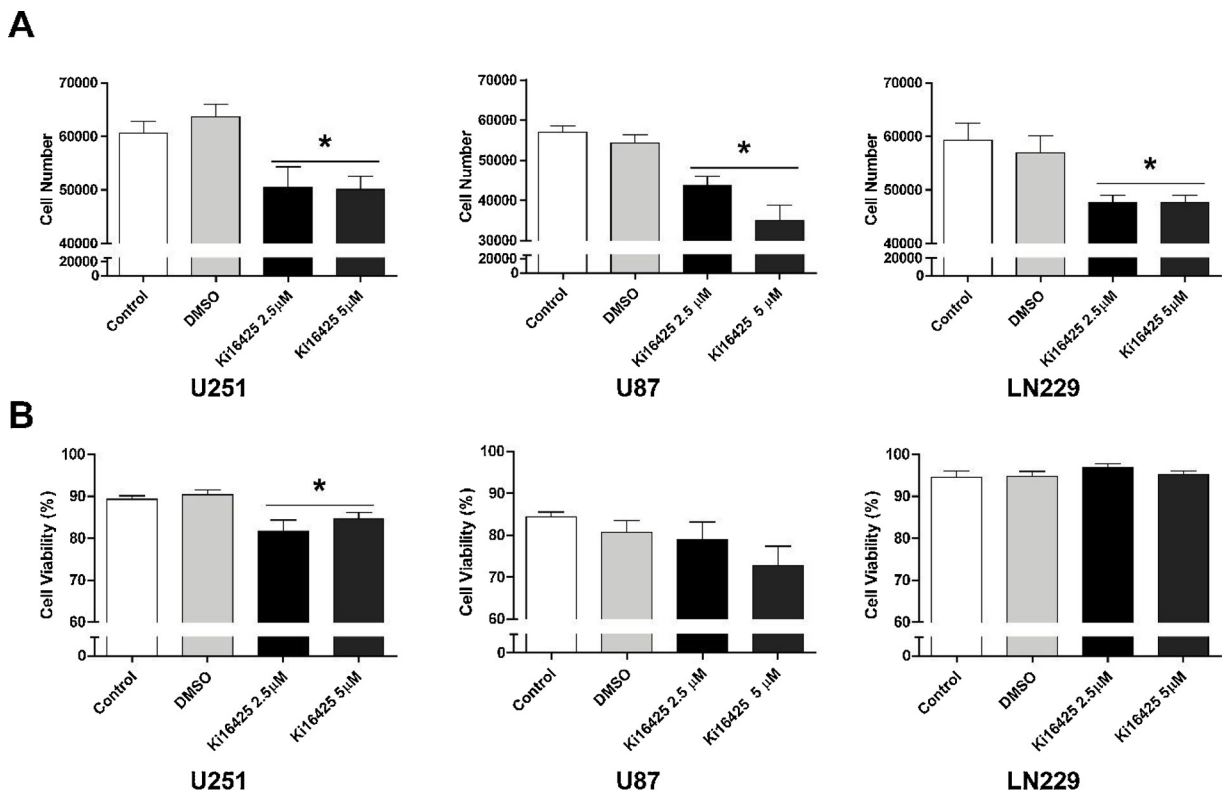

Fig. 8. LPA_1 inhibition decreased cell number in GBM cell lines. Cell number (A) and cell viability (B) in U251, U87, and LN229 were evaluated after 24 h of treatment with Ki16425 2.5 or 5 μM. Graphics represent the mean + S.E.M of 3 independent experiments by triplicate. Bonferroni post-test determined statistical difference *p < 0.05 versus control, and DMSO.

progesterone receptor (PR) at S400 (González-Arenas et al., 2015). The phosphorylation of PR on this residue induced an increase in proliferation, migration, and invasion in glioblastoma cells in vitro (González-Arenas et al., 2015; Marquina-Sánchez et al., 2016) suggesting a significant role of PKCα signaling in the nucleus by the activation of a nuclear receptor as PR that contributes to tumor development (González-Arenas et al., 2015; Lee et al., 2008). To assess if LPA_1 activation would induce PR phosphorylation S400 as a target of PKCα, we stimulated U87 and U251 cells with LPA 100 nM for 5, 15, 30 and 60 min using TPA as a positive activator of PKCα (Fig. 10A) and Ki16425 to antagonize LPA_1 activity (Fig. 10B).

We observed that LPA increased PR phosphorylation at serine 400 in both cell lines at 15 min (Fig. 10A). Interestingly, PKC activation with TPA induced PR phosphorylation from 5 to 30 min in U87 cells and until 60 min in U251 (Fig. 10A). Ki16425 blocked the phosphorylation induced by LPA at 15 min, while the treatment with only this LPA_1 receptor antagonist caused a decrease in PR basal phosphorylation that was significant compared to the control (Fig. 10B).

4. Discussion

In this work, we studied three glioblastoma cell lines to analyze PKCα activation through LPA_1. Firstly we evaluated the content of the enzyme that produces LPA, ATX (Perrakis and Moolenaar, 2014), we observed that all cell lines have a high content of this enzyme and release it to the culture media, suggesting an augmented LPA production that could contribute to LPA_1 activation. Next, we determined that LPA at low concentrations (10 and 100 nM) induced nuclear translocation of PKCα in U251 and U87 cell lines, meanwhile at high concentrations such as 1, 10 and 100μM no effect was seen. A similar effect of this lysophospholipid has been observed in migration of GBM cell lines, where 100 nM and 1μM of LPA induced higher migration compared to 10 and 100μM (Kishi et al., 2006). These results may be explained by the critical micelle concentration (CMC) of LPA; in pure water, LPA has a CMC of 0.346 mM, but at higher concentrations of salt, the CMC decreases dramatically to 0.06 mM (Li et al., 2004). It is essential to take this into account since the culture medium has abundant salts and phosphates that could reduce CMC to lower concentrations resulting in no effect of 1, 10 and 100μM of LPA, probably due to micelle formation.

We demonstrated that LPA induces in a time-dependent manner PKCα translocation to the cell membrane in three GBM cell lines. LPA induced PKCα nuclear translocation from 5 to 15 min after stimulation that finally redistributed to the cytoplasm from 30 to 60 min. Additionally, we observed that PKCα nuclear translocation is mediated through LPA_1 in U251 and U87 cells, since they did not contain LPA_3, and treatment with Ki16425 (the antagonist of LPA_1) blocked the nuclear translocation of PKCα. Although LN229 expresses LPA_3, it shows a similar pattern of nuclear translocation of the enzyme after LPA and LPA + Ki16425 treatments. Moreover, in this study, we used LPA 18:1 species, which preferentially activate LPA_1, while LPA_3 is activated by 2-acyl-LPA (Valdés-Rives and González-Arenas, 2017). However, we can't dismiss a possible additive effect of LPA_1 and LPA_3 in this cell line.

The effect of blocking LPA_1 activation through Ki16425 for 24 h showed a similar reduction in the number of the three GBM cell lines at 2.5 and 5 μM. This leads us to hypothesize that despite the expression of LPA_3 in LN229, LPA_1 may induce the main pathway through which cell number is regulated since the three cell lines decreased cell number in 20% after Ki16425 treatment. Interestingly, when PKCα was silenced in U251, U87 and LN229 there was no additive or synergistic effect with Ki16425. These data suggest that LPA_1 could induce cell number preferentially through PKCα activation. It is worth noting that the absence of PKCα in LN229 reduced cell number in 50% compared to control, while U251 and U87 decreased it in 30%. This could be due to the lesser content of PKCα in this cell line compared to U251 and U87 but a higher dependency on this kinase for proliferation.

On the other hand, cell viability was not affected in U87 and LN229

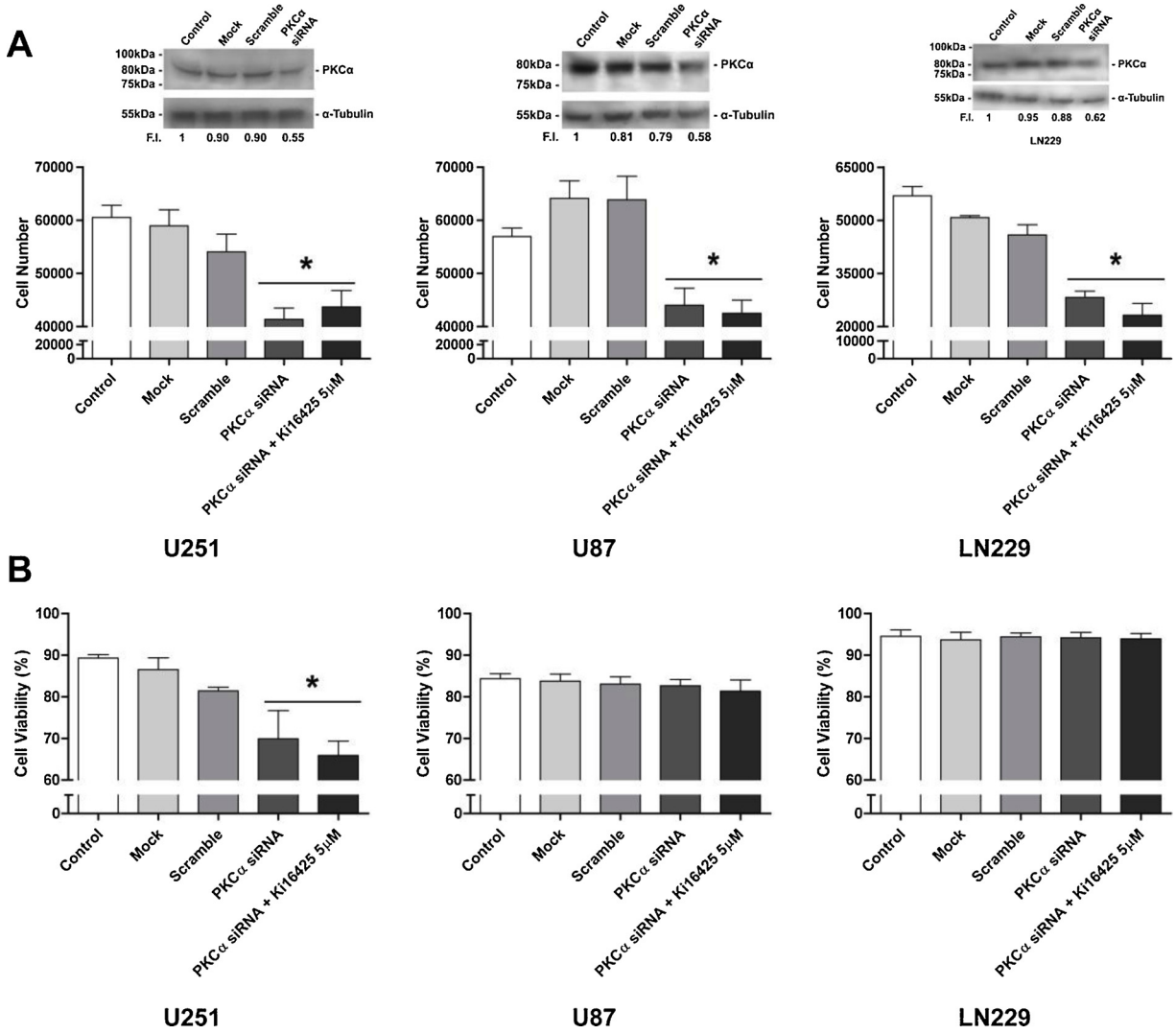

Fig. 9. LPA_1 and PKCα inhibition reduce the cell number in GBM cell lines. A) (upper panel) U251, U87, and LN229 cells were transfected with a siRNA for PKCα; Control: intact cells; Mock: cells treated only with transfection reagent without siRNA; Scramble: cells transfected with an aleatory RNA sequence. Representative Western blots for PKCα from cells lysed at 72 h after siRNA transfection (silencing) are shown. Cell number (lower panel A) and cell viability (B) were evaluated after PKCα silencing or PKCα silencing + 24 h of Ki16425 treatment. Cell cultures with mock, scramble, siRNA PKCα, and siRNA PKCα + Ki16425 were harvested at 96 h after siRNA transfection. Graphics represent the mean + S.E.M of 3 independent experiments by triplicate. Bonferroni post-test determined statistical difference *$p < 0.05$ versus control, mock and scramble.

with Ki16425 and/or silencing of PKCα, while in U251 both treatments decreased this process. This leads us to suggest that there is a difference in how these cells regulate cell number. In U251 cell death may increase after blocking LPA_1 and/or PKCα, whereas in U87 and LN229 there may be a cytostatic effect. Diverse mechanisms could be involved in regulating cell number since differences between GBM cell lines have been documented. Differentially expressed proteins between the U251 and U87 cells are associated with regulation of nicotinamide nucleotide metabolism, RNA splicing, glycolysis, and purine metabolism pathways (Li et al., 2016). In this regard participation of PKCs in the splicing regulation of proapoptotic genes has been observed in different cell lines (Revil et al., 2007); inhibition of these enzymes induce the alternative splicing of Bcl-x to generate the proapoptotic Bcl-X_S protein. However further investigation is needed to establish the mechanisms that regulate cell number and viability in U251, U87, and LN229 cells.

PKCs have been reported to target several proteins within the nucleus including histones, lamin, DNA topoisomerase, PARP, CREB, p53, GAP-43, Vitamin D3 receptor and PR among others (González-Arenas et al., 2015; Martelli et al., 2006; Trubiani et al., 2016). Our previous work in GBM cells reported that PKCα activation increased PR phosphorylation. This modification induced the receptor transcriptional activity that resulted in an increase of progesterone-induced blocking factor (PIBF) expression (Marquina-Sánchez et al., 2016), a known PR target gene, that induces glioblastoma cell proliferation (González-Arenas et al., 2015). Other genes involved in cell proliferation as EGFR and VEGF are also upregulated by PR activation in a glioblastoma cell line (Hernández-Hernández et al., 2012).

In this work, we determined that LPA_1 activation induce PR phosphorylation. The highest PR phosphorylation in U251 and U87 cells correlated with the time at which PKCα translocated to the nucleus after LPA_1 activation. Interestingly, TPA and LPA induced a different pattern of PR phosphorylation; TPA induced more sustained phosphorylation, while LPA only at 5 and 15 min in U251 and 15 min in U87. These differences could be due to the activation of PKCα; TPA induces a strong activation of PKCs without regulatory feedback (Lu et al., 1998). On the other hand, LPA induces a signaling cascade that mediates LPA_1, LPA_2 and LPA_3 homologous desensitization (Alcántara-Hernández et al., 2015) that could decrease PKCα activation and the subsequent PR phosphorylation. However, further studies are needed to establish if PR phosphorylation on S400 is due to PKCα that has been

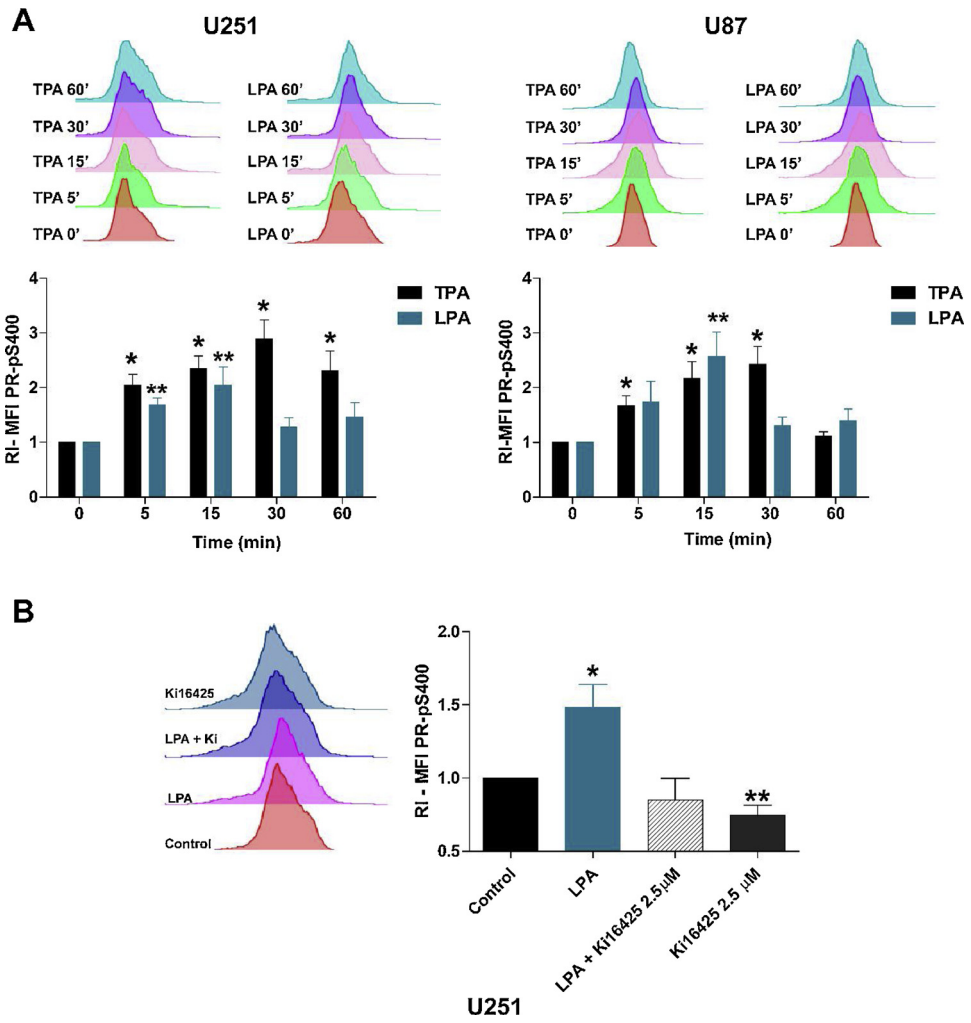

Fig. 10. LPA induces the phosphorylation of PR (S400). A) Upper panels: Representative histogram of the MFI (Mean Fluorescence Intensity) of U251 and U87 cell lines stimulated (5–60 min) with LPA 100 nM or TPA 1µM. Bottom panels: Values are expressed as relative MFI, calculated by subtracting MFI of secondary antibody control and then dividing by the MFI of T0′ of each experiment. Graphic representation, results are expressed as the mean ± S.E.M of 3 independent experiments. Bonferroni post-test determined statistical difference *p < 0.05, versus control, on cells stimulated with TPA; **p < 0.05, versus control, on cells stimulated with LPA. B) Left panel: Representative histogram of the MFI of U251 cell line with LPA 100 nM and/or Ki16425 2.5 µM. Right panel: Values are expressed as relative MFI. Graphic representation, results are expressed as the mean ± S.E.M of 3 independent experiments. Bonferroni post-test determined statistical difference *p < 0.05, versus control and LPA + Ki16425; **p < 0.05, versus control.

activated by LPA_1.

It is important to note the differences between PKCα translocation induced by TPA or LPA, as there may be mistaken conclusions about this kinase activation in physiological or pathological conditions. Additionally, the study of LPA signaling cascades in GBM is an interesting topic since it could point to different targets for therapy in this lethal cancer.

5. Conclusions

GBM tumors are highly heterogeneous, therefore finding common pathways among the different subtypes is essential. Recent studies show that LPA might be relevant for GBM biology. In three GBM cell lines, LPA induced PKCα activation through LPA1, which led to kinase nuclear translocation that impacts on cell number and viability. Further studies are needed to elucidate LPA1/PKCα relevance in GBM growth that could lead to new therapeutic targets.

Author Contributions

All authors contributed equally to this work.

Competing interests

The authors declare that they have no competing interests

Acknowledgments

This work was supported by UNAM-PAPIIT IA200718 and by Fondo Sectorial de Investigación para la Educación CB-255936/2015 CONACYT. Silvia Anahi Valdés-Rives is a doctoral student from Programa de Doctorado en Ciencias Biomédicas, Universidad Nacional Autónoma de México (UNAM), and received a Fellowship 582,548 from CONACYT. We thank Miguel Tapia-Rodríguez (Unidad de Microscopia, Instituto de Investigaciones Biomédicas, UNAM) Salvador Ramírez-Jiménez (Programa de Cáncer de mama, Instituto de Investigaciones Biomédicas, UNAM), Valeria Hansberg-Pastor, Gabriela Piña-Medina (Facultad de Química, UNAM) and Marcos García-Juárez (UAT-CINVESTAV) for their technical support.

Appendix A. Supplementary data

Supplementary material related to this article can be found, in the online version, at doi:https://doi.org/10.1016/j.biocel.2019.03.003.

References

Alcántara-Hernández, R., Hernández-Méndez, A., Campos-Martínez, G.A., Meizoso-Huesca, A., García-Sáinz, J.A., 2015. Phosphorylation and internalization of lysophosphatidic acid receptors LPA1, LPA2, and LPA3. PLoS One 10, e0140583. https://doi.org/10.1371/journal.pone.0140583.

Benesch, M.G.K., Tang, X., Maeda, T., Ohhata, A., Zhao, Y.Y., Kok, B.P.C., Dewald, J., Hitt, M., Curtis, J.M., McMullen, T.P.W., Brindley, D.N., 2014. Inhibition of autotaxin delays breast tumor growth and lung metastasis in mice. FASEB J. 28, 2655–2666. https://doi.org/10.1096/fj.13-248641.

Cameron, A.J., Procyk, K.J., Leitges, M., Parker, P.J., 2008. PKC alpha protein but not kinase activity is critical for glioma cell proliferation and survival. Int. J. Cancer 123, 769–779. https://doi.org/10.1002/ijc.23560.

Choi, J.W., Chun, J., 2013. Lysophospholipids and their receptors in the central nervous system. Biochim. Biophys. Acta - Mol. Cell Biol. Lipids 1831, 20–32. https://doi.org/10.1016/j.bbalip.2012.07.015.

do Carmo, A., Balça-Silva, J., Matias, D., Lopes, M., 2013. PKC signaling in glioblastoma. Cancer Biol. Ther. 14, 287–294. https://doi.org/10.4161/cbt.23615.

Fukushima, K., Takahashi, K., Yamasaki, E., Onishi, Y., Fukushima, N., Honoki, K., Tsujiuchi, T., 2017. Lysophosphatidic acid signaling via LPA1 and LPA3 regulates cellular functions during tumor progression in pancreatic cancer cells. Exp. Cell Res. 352, 139–145. https://doi.org/10.1016/j.yexcr.2017.02.007.

Gaits, F., Fourcade, O., Le Balle, F., Gueguen, G., Gaigé, B., Gassama-Diagne, A., Fauvel, J., Salles, J.-P., Mauco, G., Simon, M.-F., Chap, H., 1997. Lysophosphatidic acid as a phospholipid mediator: pathways of synthesis. FEBS Lett. 410, 54–58. https://doi.org/10.1016/S0014-5793(97)00411-0.

González-Arenas, A., Peña-Ortiz, M.Á., Hansberg-Pastor, V., Marquina-Sánchez, B., Baranda-Ávila, N., Nava-Castro, K., Cabrera-Wrooman, A., González-Jorge, J., Camacho-Arroyo, I., 2015. Pkcα and pkcδ activation regulates transcriptional activity and degradation of progesterone receptor in human astrocytoma cells. Endocrinology 156, 1010–1022. https://doi.org/10.1210/en.2014-1137.

Gonzalez-Gil, I., Zian, D., Vazquez-Villa, H., Ortega-Gutierrez, S., Lopez-Rodriguez, M.L., 2015. The status of the lysophosphatidic acid receptor type 1 (LPA1R). Medchemcomm 6, 13–23. https://doi.org/10.1039/C4MD00333K.

Hernández-Hernández, O.T., González-García, T.K., Camacho-Arroyo, I., 2012. Progesterone receptor and SRC-1 participate in the regulation of VEGF, EGFR and Cyclin D1 expression in human astrocytoma cell lines. J. Steroid Biochem. Mol. Biol. 132, 127–134. https://doi.org/10.1016/j.jsbmb.2012.04.005.

Kishi, Y., Okudaira, S., Tanaka, M., Hama, K., Shida, D., Kitayama, J., Yamori, T., Aoki, J., Fujimaki, T., Arai, H., 2006. Autotaxin is overexpressed in glioblastoma multiforme and contributes to cell motility of glioblastoma by converting lysophosphatidylcholine TO lysophosphatidic acid. J. Biol. Chem. 281, 17492–17500. https://doi.org/10.1074/jbc.M601803200.

Koivunen, J., Aaltonen, V., Peltonen, J., 2006. Protein kinase C (PKC) family in cancer progression. Cancer Lett. 235, 1–10. https://doi.org/10.1016/j.canlet.2005.03.033.

Lee, S.Y., Lee, H.-Y., Kim, S.D., Jo, S.H., Shim, J.W., Lee, H.-J., Yun, J., Bae, Y.-S., 2008. Lysophosphatidylserine stimulates chemotactic migration in U87 human glioma cells. Biochem. Biophys. Res. Commun. 374, 147–151. https://doi.org/10.1016/j.bbrc.2008.06.117.

Lee, S.-C., Fujiwara, Y., Liu, J., Yue, J., Shimizu, Y., Norman, D.D., Wang, Y., Tsukahara, R., Szabo, E., Patil, R., Banerjee, S., Miller, D.D., Balazs, L., Ghosh, M.C., Waters, C.M., Oravecz, T., Tigyi, G.J., 2015. Autotaxin and LPA 1 and LPA 5 receptors exert disparate functions in tumor cells versus the host tissue microenvironment in melanoma invasion and metastasis. Mol. Cancer Res. 13, 174–185. https://doi.org/10.1158/1541-7786.MCR-14-0263.

Leve, F., Peres-Moreira, R.J., Binato, R., Abdelhay, E., Morgado-Díaz, J.A., 2015. LPA induces Colon Cancer cell proliferation through a cooperation between the ROCK and STAT-3 pathways. PLoS One 10https://doi.org/10.1371/journal.pone.0139094. e0139094.

Li, Y., Gonzalez, M.I., Meinkoth, J.L., Field, J., Kazanietz, M.G., Tennekoon, G.I., 2003. Lysophosphatidic acid promotes survival and differentiation of rat Schwann cells. J. Biol. Chem. 278, 9585–9891. https://doi.org/10.1074/jbc.M213244200.

Li, Z., Mintzer, E., Bittman, R., 2004. The critical micelle concentrations of lysophosphatidic acid and sphingosylphosphorylcholine. Chem. Phys. Lipids 130, 197–201. https://doi.org/10.1016/j.chemphyslip.2004.03.001.

Li, H., Lei, B., Xiang, W., Wang, H.F.W., Liu, Y., 2016. Differences in protein expression between the U251 and U87 cell lines. Turk. Neurosurg. 1. https://doi.org/10.5137/1019-5149.JTN.17746-16.1.

Loskutov, Y.V., Griffin, C.L., Marinak, K.M., Bobko, A., Margaryan, N.V., Geldenhuys, W.J., Sarkaria, J.N., Pugacheva, E.N., 2018. LPA signaling is regulated through the primary cilium: a novel target in glioblastoma. Oncogene. 1. https://doi.org/10.1038/s41388-017-0049-3.

Louis, D.N., Ohgaki, H., Wiestler, O.D., Cavenee, W.K., Burger, P.C., Jouvet, A., Scheithauer, B.W., Kleihues, P., 2007. The 2007 WHO Classification of Tumours of the Central Nervous System. Acta Neuropathol. 114, 97–109. https://doi.org/10.1007/s00401-007-0243-4.

Louis, D.N., Perry, A., Reifenberger, G., von Deimling, A., Figarella-Branger, D., Cavenee, W.K., Ohgaki, H., Wiestler, O.D., Kleihues, P., Ellison, D.W., 2016. The 2016 World Health Organization Classification of Tumors of the Central Nervous System: a summary. Acta Neuropathol. 131, 803–820. https://doi.org/10.1007/s00401-016-1545-1.

Lu, Z., Liu, D., Hornia, A., Devonish, W., Pagano, M., Foster, D.A., 1998. Activation of protein kinase C triggers its ubiquitination and degradation. Mol. Cell. Biol. 18, 839–845. https://doi.org/10.1128/MCB.18.2.839.

Mandil, R., Ashkenazi, E., Blass, M., Kronfeld, I., Kazimirsky, G., Rosenthal, G., Umansky, F., Lorenzo, P.S., Blumberg, P.M., Brodie, C., 2001. Protein kinase Cα and protein kinase Cδ play opposite roles in the proliferation and apoptosis of glioma cells. Cancer Res. 61, 4612–4619.

Marquina-Sánchez, B., González-Jorge, J., Hansberg-Pastor, V., Wegman-Ostrosky, T., Baranda-Ávila, N., Mejía-Pérez, S., Camacho-Arroyo, I., González-Arenas, A., 2016. The interplay between intracellular progesterone receptor and PKC plays a key role in migration and invasion of human glioblastoma cells. J. Steroid Biochem. Mol. Biol. https://doi.org/10.1016/j.jsbmb.2016.10.001.

Martelli, A.M., Evangelisti, C., Nyakern, M., Manzoli, F.A., 2006. Nuclear protein kinase C. Biochim. Biophys. Acta (BBA)-Molecular Cell Biol. Lipids. 1761, 542–551. https://doi.org/10.1016/j.bbalip.2006.02.009.

Mills, G.B., Moolenaar, W.H., 2003. The emerging role of lysophosphatidic acid in cancer. Nat. Rev. Cancer 3, 582–591. https://doi.org/10.1038/nrc1143.

Mooleenar, W.H., 2006. Development of our current understanding of bioactive lysophospholipids. Ann. N. Y. Acad. Sci. 905, 1–10. https://doi.org/10.1111/j.1749-6632.2000.tb06532.x.

Ostrom, Q.T., Gittleman, H., Truitt, G., Boscia, A., Kruchko, C., Barnholtz-Sloan, J.S., 2018. CBTRUS statistical report: primary brain and other central nervous system tumors diagnosed in the United States in 2011–2015. Neuro. Oncol. 20, iv1–iv86. https://doi.org/10.1093/neuonc/noy131.

Perrakis, A., Moolenaar, W.H., 2014. Autotaxin: structure-function and signaling. J. Lipid Res. 55, 1010–1018. https://doi.org/10.1194/jlr.R046391.

Revil, T., Toutant, J., Shkreta, L., Garneau, D., Cloutier, P., Chabot, B., 2007. Protein kinase C-dependent control of Bcl-x alternative splicing. Mol. Cell. Biol. 27, 8431–8441. https://doi.org/10.1128/MCB.00565-07.

Seo, E.J., Kwon, Y.W., Jang, I.H., Kim, D.K., Lee, S.I., Choi, E.J., Kim, K., Suh, D., Lee, J.H., Choi, K.U., Lee, J.W., Mok, H.J., Kim, K.P., Matsumoto, H., Aoki, J., Kim, J.H., 2016. Autotaxin regulates maintenance of ovarian Cancer stem cells through lysophosphatidic acid-mediated autocrine mechanism. Stem Cells 34, 551–564. https://doi.org/10.1002/stem.2279.

Steinberg, S.F., 2008. Structural basis of protein kinase C isoform function. Physiol. Rev. 88, 1341–1378. https://doi.org/10.1152/physrev.00034.2007.

Tabuchi, S., 2015. The autotaxin-lysophosphatidic acid–lysophosphatidic acid receptor cascade: proposal of a novel potential therapeutic target for treating glioblastoma multiforme. Lipids Health Dis. 14, 56. https://doi.org/10.1186/s12944-015-0059-5.

Trubiani, O., Guarnieri, S., Diomede, F., Mariggiò, M.A., Merciaro, I., Morabito, C., Cavalcanti, M.F.X.B., Cocco, L., Ramazzotti, G., 2016. Nuclear translocation of PKCα isoenzyme is involved in neurogenic commitment of human neural crest-derived periodontal ligament stem cells. Cell. Signal. 28, 1631–1641. https://doi.org/10.1016/J.CELLSIG.2016.07.012.

Valdés-Rives, S.A., González-Arenas, A., 2017. Autotaxin-lysophosphatidic acid: from inflammation to Cancer development. Mediators Inflamm. 2017, 9173090. https://doi.org/10.1155/2017/9173090.

Wegman-Ostrosky, T., Reynoso-Noverón, N., Mejía-Pérez, S.I., Sánchez-Correa, T.E., Alvarez-Gómez, R.M., Vidal-Millán, S., Cacho-Díaz, B., Sánchez-Corona, J., Herrera-Montalvo, L.A., Corona-Vázquez, T., 2016. Clinical prognostic factors in adults with astrocytoma: historic cohort. Clin. Neurol. Neurosurg. 146, 116–122. https://doi.org/10.1016/j.clineuro.2016.05.002.

Yung, Y.C., Stoddard, N.C., Chun, J., 2014. LPA receptor signaling: pharmacology, physiology, and pathophysiology. J. Lipid Res. 55, 1192–1214. https://doi.org/10.1194/jlr.R046458.

Yung, Y.C., Stoddard, N.C., Mirendil, H., Chun, J., 2015. Lysophosphatidic acid signaling in the nervous system. Neuron 85, 669–682. https://doi.org/10.1016/J.NEURON.2015.01.009.

Zhang, H., Xu, X., Gajewiak, J., Tsukahara, R., Fujiwara, Y., Liu, J., Fells, J.I., Perygin, D., Parrill, A.L., Tigyi, G., Prestwich, G.D., 2009. Dual activity lysophosphatidic acid receptor Pan-Antagonist/Autotaxin inhibitor reduces breast Cancer cell migration in vitro and causes tumor regression in vivo. Cancer Res. 69, 5441–5449. https://doi.org/10.1158/0008-5472.CAN-09-0302.